NUMERICAL SIMULATION OF THE FLOW IN A SYMMETRICAL DEEP-BOWL COMBUSTION CHAMBER OF A DIESEL ENGINE CYLINDER DURING THE COMPRESSION STROKE

BY

M. S. EL-Kady[1], H. J. Mascheck[2], & A. Hoche[3]

(Received Sep. 14, 1987, accepted Dec. 1987)

خلاصة ـ هذا البحث يشرح ويقدم نموذج عددى وطريقة عددية لاستنباط حركة الهواء الدوامية الغير مستقرة فى غرفة احتراق اسطوانية متماثلة حول المحور فى ماكينة ديزل ذات حقن مباشر خلال شوط الانضغاط . وتكونت المعادلات التى تصيغ هذه الحركة من معادلة الاستمرار ومعادلات كمية الحركة التى صيغت فى نظام احداثيات متحركة . وخلال عملية النمذجة العددية استخدمت طريقة الفروق المحددة التى استخدمت فيها شبكتان مرحلتان ثنائيتى الابعاد وذلك لكل من المتغيرات المتجه والمتغيرات العياسة وقد تم صياغة الضغط بطريقة غير مباشرة عن طريقة معادلة الاستمرار التى أستخدمت فيها طريقة الاتجاه المتغير الغير مربع (ADI) وذلك لعملية تصحيح الضغط بواسطة التكرار . وقد تم حساب مثال عددى على أحدى ماكينات الديزل الصغيرة أظهر أهم خواص السريان للهواء داخل الاسطوانة وأثبت أن هذه الطريقة العددية يمكن أن تستخدم بكفاءة عالية لاستنباط حركة الهواء ثلاثية الابعاد فى غرف الاحتراق الغير مركزية .

ASBTRACT - This paper describes a method for predicting the unsteady axisymmetric air flow in a deep bowel combustion chamber of the direct injection diesel engine during the compression stroke. The governing equations are the continuity and the momentum equations. A movable coordinate system is used in which these equations are transformed. For the numerical simulation a finite difference algorithm developed by the authors is used in which two different staggard, two dimensional and movable grids are used for the vector and scalar variables. The pressure is described indirectly through the continuity equation and the ADI-method is used for the interation of it. A computer program EBSTR is made and used for the numerical computation. The computed results which are drawn with the use of EBSTR are used to show the main characteristics of the flow.

1- INTRODUCTION

For many years research is being done on the air flow in the cylinder space of reciprocating combustion engines. This field is very important, as the fuel mixing to the air, ignition and combustion as well as the heat transfer to the cylinder walls are substantially influenced by the air motion in the cylinder specially during the latest portion of the compression stroke between 30° before top dead center (TDC) and the TDC. However the flow in the cylinder is unsteady and turbulent and has not been clarified fully.

1- Lecturer, Mech. Power Dept., Faculty of Engineering, Mansoura University
2- Professor, Institute of Fluid Mechanics, University of Dresden, East Germany (GDR)
3- Professor,head of the institute of Internal Combustion Engines, University of Dresden, East Germany (GDR)

Several different approaches have been taken in computing the flow and combustion processes in the reciprocating combustion engines. Gosman et al [1]. Ramos et al [2] computed the flow during the intake stroke treating it as an axi-symmetric three dimensional flow and using a two equation model for turbulence. Griffin et al [3,4] computed two dimensional laminar flow in a cylinder at low Reynold numbers. Seppen [5] developed a two dimensional model to represent the air motion during the compression stroke of an engine with flat piston.

In the present study the turbulent flow generated by the movement of the piston from BDC to TDC during compression stroke in a deep bowl axisymmetric combustion chamber in the piston is predicted. The prediction was carried out using a finite difference algorithm developed by the authors [6] to solve the continuity and momentum equations. This paper describes this algorithm and gives the result of sample calculation.

2- MATHEMATICAL MODEL

2.1. Governing Equations

In the formulation a cylindrical coordinates (r,0,z) has been employed, in which velocity components are denoted by u,v,w.. as shown in Fig.1. Assuming that the instantaneous fluid density is spatially uniform over the flow field but depends on time, the momwntum and continuity equations for the two dimensional unsteady inviscid axisymmetric flow will be as follows :

$$\frac{\partial u}{\partial t} + u\frac{\partial u}{\partial r} - \frac{v^2}{r} + w\frac{\partial u}{\partial z} + \frac{\partial p}{\partial r} = 0 \qquad (1)$$

$$\frac{\partial v}{\partial t} + u\frac{\partial v}{\partial r} + \frac{u\,.\,v}{r} + w\frac{\partial v}{\partial z} = 0 \qquad (2)$$

$$\frac{\partial w}{\partial t} + u\frac{\partial w}{\partial r} + w\frac{\partial w}{\partial z} + \frac{\partial p}{\partial z} = 0 \qquad (3)$$

$$\frac{1}{r}\frac{\partial u.r}{\partial r} + \frac{\partial w}{\partial z} + \frac{1}{\rho}\frac{d\rho}{\partial t} = 0 \qquad (4)$$

where p is the pressure divided by the density.

2.2. Integration area

Figs. 1,2 show the integration area with its boundaries which consists of the axis, cylinder head, cylinder wall, piston crown, bowl wall and bowl bottom.

During the motion of the piston in a fixed z coordinate the boundaries of the integration area will vary with the time, to avoid an incomplete coverage of the wall boundaries on the computational grid which will be discussed in 3.3. a movable coordinate z'is used in the axial direction to make the boundaries of the integration area time independent where:

$$z' = \frac{z}{h}\,c_1 \qquad 0 \le z' \le c_1\,, \qquad 0 \le z \le h$$

$$z' = z + c_1 - h \qquad c_1 \le z' \le c_1 + b_1,\ h \le z \le h + b_1$$

The governing equations will be transformed to the time movable coordinate system in which every point has an axial velocity in the cylinder, that is the same velocity of the grid point w_g in figure 2. The time derivative for the moving coordinate will take the following form :

$$\left.\frac{\partial}{\partial t}\right|_{mov} = \left.\frac{\partial}{\partial t}\right|_{fixed} + w_g \frac{\partial}{\partial z} \qquad (5)$$

where $w_g = \frac{z}{h} w_p$ for $0 \leq z \leq h$

$w_g = w_p$ for $h \leq z \leq h + b_l$

This will change the governing equations (1)-(3) by only an excess derivative term in the convection form in the axial direction.

2.3. The Boundary and Initial Conditions

The boundary conditions will be expressed as follows :

$u = 0$, $v = 0$, $\frac{\partial w}{\partial r} = 0$ and $\frac{\partial p}{\partial r} = 0$ at the axis where $r = 0$.
$u = 0$ at the cylinder and bowl walls, $w = 0$ at the cylinder head and $w = w_p$ at the piston crown and the bowl bottom.

The initial conditions are given to the quantities at the time of inlet valve closing as a forced vortex having a swirl ratio ω_o which is assumed to be constant in the axial direction.

3. SOLUTION ALGORITHM

3.1. Reformulation of the Governing Equations

The momentum equations (1)-(3) in the movable coordinate system can be expressed with the use of the operators N, G, and the vecor u which will be discussed later in the following form :

$$\frac{\partial \vec{u}}{\partial t} = N(\vec{u}, w_g) - Gp \qquad (6)$$

where $\vec{u} = \begin{bmatrix} u \\ v \\ w \end{bmatrix}$

With the same procedure and the use of the operator D the continuity equation (4) will be expressed as follows :

$$D\vec{u} + \frac{1}{\rho} \frac{d\rho}{dt} = 0 \qquad (7)$$

The definitions of the convection operator N, the gradient operator G and the divergent operator D are obtained from the comparison of equations (6) and (7) with equations (1)-(5). This will give with the use of $\vec{u}$, g and f for the vector and scalar quantities, the operators N, G and D as follows :

$$N(\vec{u}, g) = -u \frac{\partial u}{\partial r} + (g - w) \frac{\partial u}{\partial z} + \begin{bmatrix} v^2/r \\ -u.v/r \\ 0 \end{bmatrix} \qquad (8)$$

$$Gp = \begin{bmatrix} \partial f / \partial r \\ 0 \\ \partial f / \partial z \end{bmatrix} \qquad (9)$$

$$D\vec{u} = \frac{1}{r} \frac{\partial (u.r)}{\partial r} + \frac{\partial w}{\partial z} \qquad (10)$$

3.2. Method of Solution

For the known pressure field it is so easy to solve the momentum equations and get the velocity components, but to know the pressure field that is the problem. The pressure will be here described indirectly through the continuity equation, then the correct pressure field is substituted in the momentum equations, the resultant velocities must satisfy the continuity equation. This procedure will be used as follows:

The simplest explicit one direction method is used for the time derivatives in equations (6) by which the velocity $\vec{u}$ at the time $t+\delta t$ is calculated from the velocity $\vec{u}'$ at the time t as follows :

$$\vec{u} = \vec{u}' + \frac{\partial \vec{u}'}{\partial t} \delta t \qquad (11)$$

From the fact that the new $\vec{u}$ at the time $t + \delta t$ must satisfy the continuity equation (7) then by substituting $\vec{u}$ in equation (7) it will take the following form

$$D(\vec{u}' + \delta t \frac{\partial \vec{u}'}{\partial t}) + \frac{1}{\varrho} \frac{d\varrho}{dt} = 0 \qquad (12)$$

Taken into consideration equation (6) and with the use of the relation

$$\vec{q} = \vec{u}' + \delta t \, N(\vec{u}, w_g) \qquad (13)$$

For the convection term and also $P = p.\delta t$ equation (12) will give for the pressure the following equation

$$DGP = D\vec{q} + \frac{1}{\varrho} \frac{d\varrho}{dt} \qquad (14)$$

Equation (14) is an elliptic equation from the type of poission's equation. It is used to calculate p by the known right hand side. This equation will be solved by iteration and the ADI-method [7] will be used for this purpose.

By the known resultant value of P the velocity $\vec{u}$ can be calculated by the following equation

$$\vec{u} = \vec{q} - GP \qquad (15)$$

3.3. Discretisation of the Differential Equations

For the discretisation of the governing equations two different two-dimensional staggard grids in the way discussed by Stephens et al [8] are used for the vector and scalar variables as shown in figure 2. The crosses (+) represent the points of the grid $\mathfrak{R}_G$ for the vector field and the points (.) represent the points of the grid $\tilde{\mathfrak{R}}_G$ for the scalar field. The calculation of the convection terms and the pressure gradient will be at the points of the grid $\mathfrak{R}_G$ and the satisfaction of the continuity equation will be at the points of the grid $\tilde{\mathfrak{R}}_G$.

Variable axial spacing is used to allow for the change in the distance between the cylinder head and the piston crown, while a fixed grid system is used for the space in the piston bowl. The number of the axial nodes during the compression was made variable to avoid the extremely small spacing between the node pointe and to make the ratio of the axial spacing in the head piston space to that in the piston bowl within the range of 1.5 to 1/1.5. This condition was satisfied either by doubling the spacing in the head piston space or by halfing it in the piston bowl.

To express the discrete operators which are used in equations (13)-(15)

and also in the boundary conditions without making many special forms, the following relations will be taken into consideration :

$$(a)^+ = \begin{cases} a & \text{for } a > 0 \\ 0 & \text{for } a \leq 0 \end{cases} \quad , \quad d_k = \begin{cases} d_c & \text{for } 1 \leq k < L_3 \\ d_b & \text{for } L_3 \leq k \leq L_4 \end{cases}$$

$$w_{gk} = \begin{cases} \dfrac{(k-1)}{(L_3-1)}\, w_p & \text{for } k \leq L_3 \\ w_p & \text{for } k \geq L_3 \end{cases}$$

$$r_i = (i-1)\, d_r \quad , \quad \tilde{r}_i = (i-\tfrac{1}{2})\, d_r$$

with these relations the convection operator N takes the form

$$[N(\vec{u},w_g)]_{i,k} = \frac{1}{d_r}\left[(u_{i,k})^+ \cdot (\vec{u}_{i-1,k}-\vec{u}_{i,k}) + (-u_{i,k})^+ \cdot (\vec{u}_{i+1,k}-\vec{u}_{i,k})\right] + \frac{1}{d_{k-1}}(w_{i,k}-w_{gk})^+ \cdot (\vec{u}_{i,k-1}-\vec{u}_{i,k}) + \frac{1}{d_k}(w_{gk}-w_{i,k})^+ \cdot (\vec{u}_{i,k+1}-\vec{u}_{i,k}) + \frac{1}{r_i}\begin{bmatrix} v^2_{i,k} \\ -u_{i,k}\cdot v_{i,k} \\ 0 \end{bmatrix} \qquad (16)$$

and the gradient field Gf will be

$$[Gf]_{i,k} = \frac{1}{d_r\left(\frac{1}{d_{k-1}}+\frac{1}{d_k}\right)} \begin{bmatrix} d_{k-1}(f_{i,k}-f_{i-1,k}) + d_k(f_{i,k-1}-f_{i-1,k-1}) \\ 0 \\ d_r(f_{i,k}+f_{i-1,k}-f_{i,k-1}-f_{i-1,k-1}) \end{bmatrix} \qquad (17)$$

Figure 3 shows the values of the function f which is used in equation (17) to calculate the gradient field f at the point $p_{i,k} \in \Omega_G$. To make the normal component at the boundary point equal zero, the values of the scalar field f outside the integration area was make equal to the values of it at the inside points (mirror image at the boundary) and at the point $p_{i,k}$ at the axis where r=0 the scalar field was made to take the value p(r,z)=-p(-r,z).

Figure 4 shows the velocity components which were used to calculate the discrete value of the diverging operator $D\vec{u}$ at the point $p_{i,k} \in \bar{\Omega}_G$ according to the definition shown in equation (10) as follows :

$$[D\vec{u}]_{i,k} = \frac{1}{2\tilde{r}_i}\left[\frac{r_{i+1}}{d_r}(u_{i+1,k}+u_{i+1,k+1}) - \frac{r_i}{d_r}(u_{i,k}+u_{i,k+1})\right] + \frac{r_{i+1}}{d_k}(w_{i+1,k+1}-w_{i+1,k}) + \frac{r_i}{d_k}(w_{i,k+1}-w_{i,k}) \qquad (18)$$

4- NUMERICAL EXAMPLE

The computer program EBSTR is written for this system in FORTRAN and the detailed discussion is found in ref. [9]. The computation was made for a small size direct injection diesel engine having a cylinder diameter of 120 mm, a stroke of 102.8 mm, a ratio of crank arm to connecting rod of 0.27, cylinder height at BDC is 120 mm, diammeter ratio of bowl to cylinder is 0.4, bowl height is 37.5 mm, speed of 2400 rpm and $\omega_0 = 0.6$.

Figure 5 shows the resultant velocity in the r-z plane by way of vectors and contours respectively for different crank angles from 120° after BDC to 180° (TDC) for the compression stroke. The points show the measured positions while the lines indicate the magnitude and direction of the velocities. The velocity distribution in this figure is drawn relative to the piston surface. Figure 5 shows that as the piston goes up the air is forced to flow into the bowl and forms a radial inward squish flow. In the earlier stages of this flow the squish air jet is strongly bent in the bowl entrance owing to a centrifugal force due to the swirl, and finally a clockwise vortex flow is produced at the TDC.

Figure 6 shows the accopanied pressure difference of the flow. It is well known from the figure that the maximum difference in the pressure takes about 5% of the absolute pressure which makes the assumption that the instantaneous fluid density is spatially uniform over the flow field to be valid.

Figure 7 shows the tangential velocity for 120, 160, 170 and 180° CA during the compression stroke. The tangential velocity is proportional to the radius at the moment when the inlet valve closes. This velocity becomes always high at the bowl periphery as the compression proceeds. It increases from 4.8 m/s at BDC to 8.4 m/s at 120°CA after BDC to about 13.2 m/s at the TDC. This increase is about 300% during the compression stroke. In the piston cavity and owing to the secondary flow in the r-z plane the profile of the periphery velocity remains no longer in a simple solid body rotation.

5- CONCLUSIONS

In the present study a finite difference method has been used for performing a numerical simulation of the in-cylinder flow to enable prediction of the fluid flow in the engine cylinders. This method has been applied to simulate the two dimensional air flow in the axisymmetric deep-bowl combustion chamber diesel engine during the compression stroke. The results are satisfactory well reproducing global features of the fluid motions. Thus it can be safely said that the numerical simulation method is a powerful tool to explore the in-cylinder unsteady flow and it can be also extended and used to simulate the fully three-dimensional in-cylinder unsteady flow during the four strokes.

6- NOMENCLATURE

b_1	bowl height (depth)
c_1	total cylinder length = h at BDC
d_b , d_c	grid spacing in z-direction in bowl and cylinder
d_r	grid spacing in r-direction
D	Divergent operator
f	scalar field
G	gradient operator
h	piston position from the cylinder top
$L_1,...,L_4$	number of mish points in z and r directions

N	convection operator
p	pressure / density
P	p.δt
t	time
$\vec{u}$	velocity vector
u,v,w	radial, tangential and axial velocity components
z,z	fixed and movable axial coordinates
ρ	density
ϕ	crank angle
ω_o	swirl ratio, the ratio of swirl angular velocity to that of the engine shaft

7- REFERENCES

1- Gosman, A.D. and John, R.J.R., SAE paper No. 800091 (1980)

2- Ramos, J.I., Humphery, J.A.C. and Sirignano, N.A., SAE paper No. 790356 (1979)

3- Griffin, M.D., Anderson, J.D., Diwaker, R., Navier-Stokes solutions of flow field in an I.C.E. AIAA Journal, Vol 14 Dec. 1976 pp 1665-1666.

4- Diwakar, R., Anderson, J.D., Griffin, M.D., Inviscid solutions of the flow field in an I.C.E. AIAA Journal, Vol. 14, Dec. 1976, pp 1667-1668.

5- Seppen, J.J., A study of flow field phenomena in I.C.E. ph.D. thesis, TH Delft, october 1982.

6- EL Kady, M.S., Berechnung symmetrischer und unsymmetrischer Zylinder-Brennraum-Strömungen in Dieselmotoren beim Verdichtungshub, Dissertation, TU Dresden March 1985.

7- Peaceman, D.W., Rachford, H.H., The numerical solution of parabolic and elliptic differential equations, J. Soc. Indust. Appl. Math. 3, 28-41, 1955.

8- Stephens, A.S., Bell, J.B., Solomon, J.M., A finite difference formulation for the incompressible N. S. Equation, J. of computational physics, Vol. 53 (1984) pp 152-172

9- EL Kady, M.S., Anleitung zur Nutzung der Programme fur die Berechnung der Zylinder-Brennraum-Strömungen in Dieselmotoren beim Verdichtungshub. Bericht No. 656, TU Dresden Sektion 12, WB Strömungstechnik.

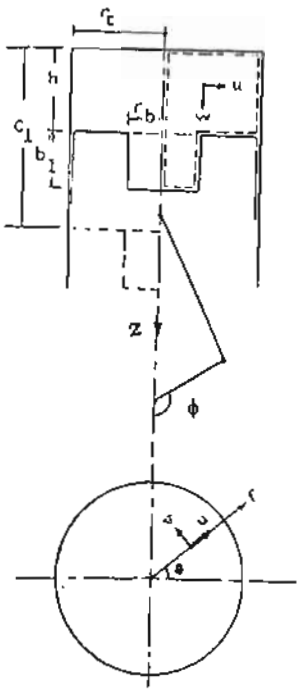

Fig. 1 Integration area

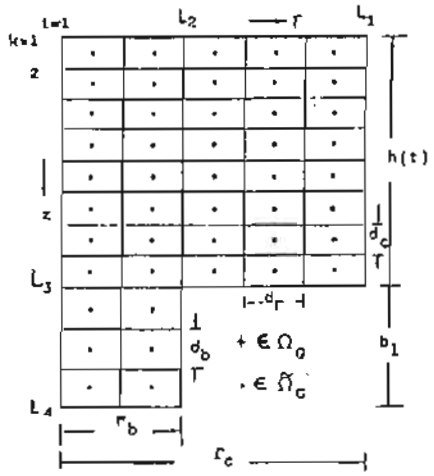

Fig. 2 Computational grid arrangement

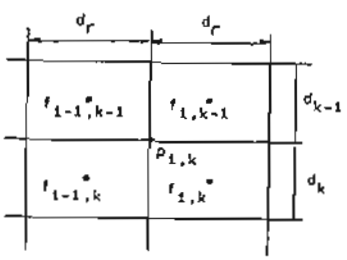

Fig. 3 The values of the function f which is used to calculate the gradient field Gf

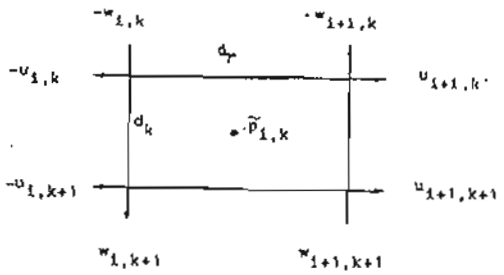

Fig. 4 The velocity components which is used to calculate the discrete value of $D\vec{u}$

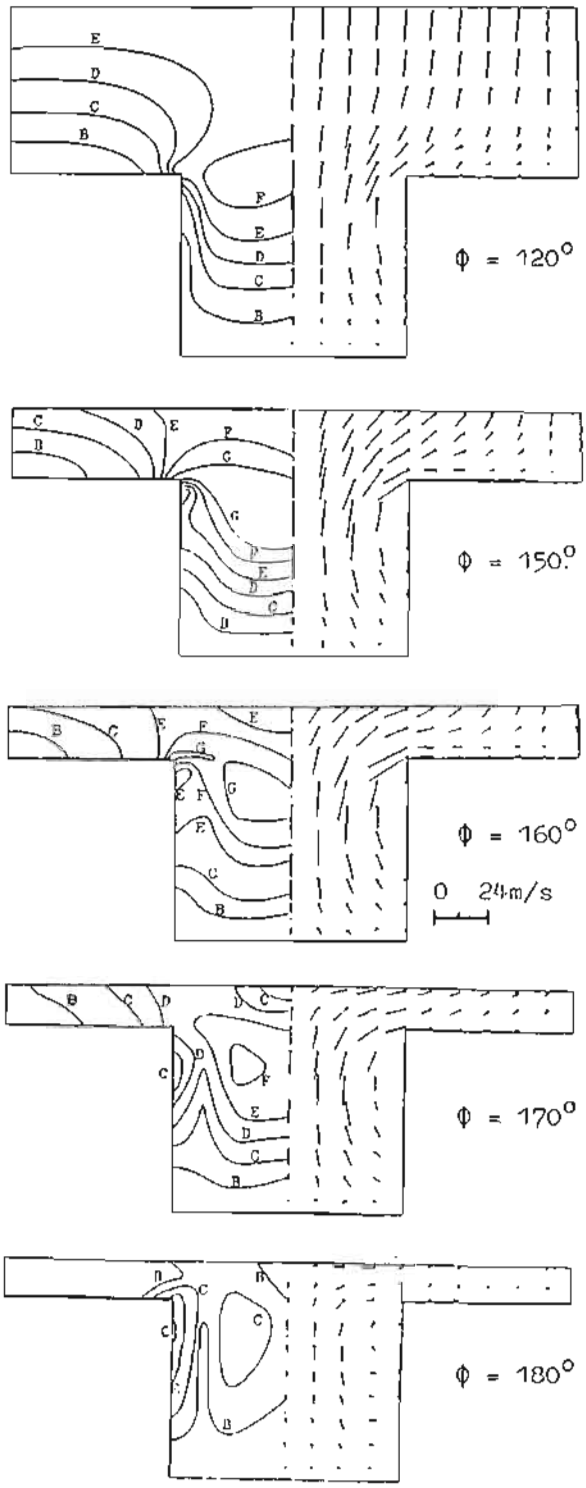

Fig. 5 The resultant velocity in the r-z plane by way of vectors and contours

B = 2,4
C = 4,8
D = 7,2
E = 9,6
F = 12,0
G = 14,4
H = 16,8 m/s

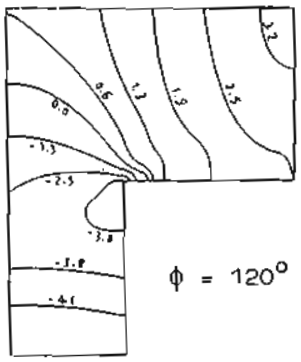

Fig. 6

The pressure difference of the flow for 120° - 180°CA after BDC during compression stroke

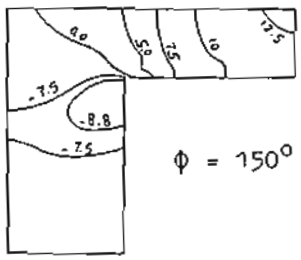

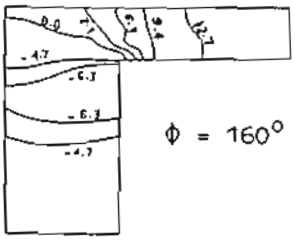

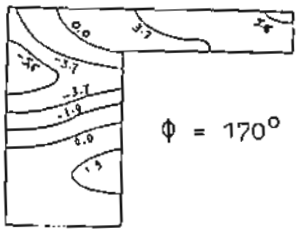

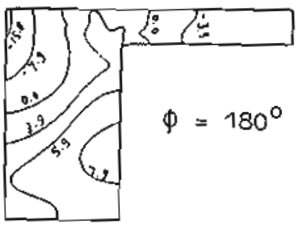

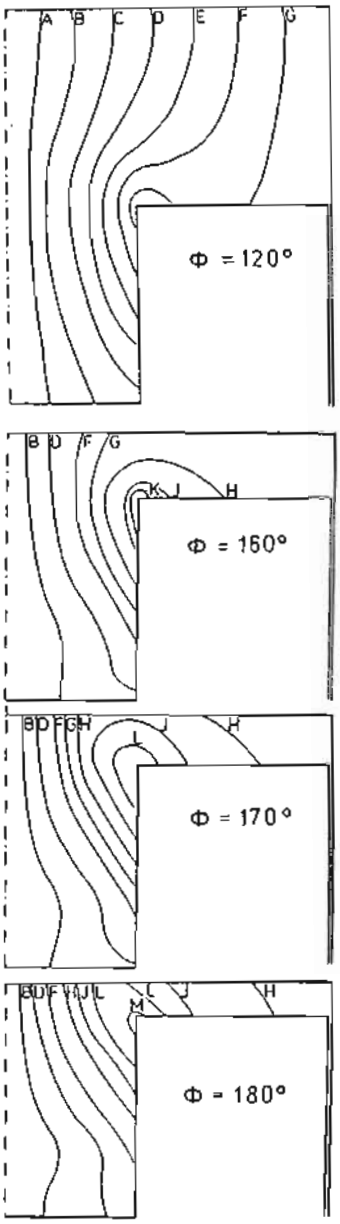

Fig. 7

The tangential velocity for 120° - 180°CA after BDC during compression stroke

O = 0.0
A = 1.2
B = 2.4
C = 3.6
D = 4.8
E = 6.0
F = 7.2
G = 8.4
H = 9.6
J = 10.8
K = 11.4
L = 12.0
M = 13.2 m/s